available at www.sciencedirect.com

SCIENCE DIRECT®

journal homepage: www.elsevier.com/locate/biochempharm

Characterization of the melatoninergic MT_3 binding site on the NRH:quinone oxidoreductase 2 enzyme

François Mailliet[a], *Gilles Ferry*[a], *Fanny Vella*[a], *Sylvie Berger*[a], *Francis Cogé*[a], *Pascale Chomarat*[a], *Catherine Mallet*[a], *Sophie-Pénélope Guénin*[a], *Gérald Guillaumet*[b], *Marie-Claude Viaud-Massuard*[c], *Saïd Yous*[d], *Philippe Delagrange*[e], *Jean A. Boutin*[a,*]

[a] *Division de Pharmacologie Moléculaire et Cellulaire, Institut de Recherches Servier, 125 Chemin de Ronde, 78290 Croissy-sur-Seine, France*

[b] *Institut de Chimie Organique et Analytique (ICOA), UMR-CNRS 6005, Université d'Orléans, rue de Chartres, BP 6759, 45067 Orléans Cedex 02, France*

[c] *Université François Rabelais, EA3857 SPOT Laboratoire de Physicochimie Organique et Thérapeutique, UFR des Sciences Pharmaceutiques, 31 Avenue Monge, 37200 Tours, France*

[d] *Laboratoire de Chimie Thérapeutique EA1043, Faculté des Sciences Pharmaceutiques et Biologiques, rue du Professeur Laguesse, BP 83, 59006 Lille Cedex, France*

[e] *Département des Sciences Expérimentales, Institut de Recherches Servier, 11 rue de Moulineaux, 92150 Suresnes, France*

ARTICLE INFO

Article history:
Received 9 August 2005
Accepted 29 September 2005

Keywords:
Melatonin
Quinone reductase 2
MT_3
Molecular pharmacology
Inhibitors
Binding

Abbreviations:
2-I-MLT, 2-iodomelatonin
2-[^{125}I]-MLT, 2-[^{125}I]-iodomelatonin
2-[^{125}I]-MCA-NAT, 2-[^{125}I]-iodo-5-methoxycarbonylamino-*N*-acetyltryptamine
AFMK, N^1-acetyl-N^2-formyl-5-methoxy-kynurenamine

ABSTRACT

Melatonin acts through a series of molecular targets: the G-protein coupled receptors, MT_1 and MT_2, and a third binding site, MT_3, recently identified as the enzyme NRH:quinone oxydoreductase 2 (QR2). The relationship between the multiple physiological functions of melatonin and this enzyme remains unclear. Because of the relationship of QR2 with the redox status of cells, these studies could bring the first tools for a molecular rationale of the antioxidant effects of melatonin. In the present paper, we used a QR2-stably expressing cell line and hamster kidneys to compare the 2-[^{125}I]-iodomelatonin and 2-[^{125}I]-iodo-5-methoxycarbonylamino-*N*-acetyltryptamine binding data, and to characterize the MT_3 binding site. We designed and tested compounds from two distinct chemicals series in a displacement assay of the two MT_3 ligands, 2-[^{125}I]-iodomelatonin and 2-[^{125}I]-iodo-5-methoxycarbonylamino-*N*-acetyltryptamine from their cloned target. We also tested their ability to inhibit QR2 catalytic activity. These compounds were separated into two classes: those that bind within the catalytic site (and being inhibitors) and those that bind outside it (and therefore not being inhibitors). Compounds range from potent ligands (K_i = 1 nM) to potent inhibitors (14 nM), and include one compound [NMDPEF: *N*-[2-(2-methoxy-6H-dipyrido[2,3-a:3,2-e]pyrrolizin-11-yl)ethyl]-2-furamide] active on both parameters in the low nanomolar range. To dissect the physio-pathological pathways in which QR2, MT_3 and melatonin meet, one needs more compounds binding to MT_3 and/or inhibitors of QR2 enzymatic activity. The compounds described in the present paper are new tools for such a task.

* *Corresponding author*. Tel.: +33 1 55 72 27 48; fax: +33 1 55 72 28 10.
E-mail address: jean.boutin@fr.netgrs.com (J.A. Boutin).

0006-2952/$ – see front matter © 2005 Elsevier Inc. All rights reserved.
doi:10.1016/j.bcp.2005.09.030

AMK, N^1-acetyl-5-methoxykynurenamine
BNAH, dihydrobenzylnicotamide
CHO cells, Chinese Hamster Ovary
FAD, flavin adenine dinucleotide
hQR2-FAD, oxidative state of the FAD cofactor into hQR2 protein
hQR2-$FADH_2$, reductive state of the FAD cofactor into hQR2 protein
MCA-NAT, 5-methoxycarbonylamino-N-acetyltryptamine
MLT, melatonin
NAS, N-acetylserotonin
hQR2, human quinone reductase 2
NRH, dihydronicotinamide riboside
QR1, quinone reductase 1 (NQO1)
TCA, trichloroacetic acid
TFA, trifluoroacetic acid

1. Introduction

Melatonin (MLT) is a neurohormone derived from serotonin that is almost exclusively synthesized in the pineal gland [1]. This indoleamine exerts its central and peripheral effects through an yet undetermined number of receptors or molecular targets [2]. The best described receptors are the two MLT high affinity binding G-proteins coupled receptors (GPCR) called MT_1 and MT_2 [3]. The comparative pharmacology of the human and ovine MLT receptors has been established [4,5]. Another binding site, MT_3, which presents a low affinity binding for the radiolabelled 2-[^{125}I]-iodomelatonin (2-[^{125}I]-MLT) has been described [6–9]. Although it had been suggested in early reports, it is not longer believed to be coupled to G-proteins [10,11]. A more specific radioligand, 2-[^{125}I]-iodo-5-methoxycarbonylamino-N-acetyltryptamine (2-[^{125}I]-MCA-NAT), has been shown to discriminate MT_3 from the G-protein coupled MT_1 and MT_2 receptors [12–14]. The MT_3 site displays fast ligand association/dissociation kinetics when compared to standard seven-transmembrane domain, G-protein coupled receptor biochemistry [6,9,12]. The physiological role of MT_3 site has not yet been identified, although a connexion between intraocular pressure and the MT_3 ligand, 5-MCA-NAT has been reported [15–17].

The MT_3 binding site has been purified and characterized from hamster kidneys [13]. Its molecular properties, and the observation that a mouse strain depleted in the quinone reductase 2 (QR2) gene does not exhibit any 2-[^{125}I]-MCA-NAT specific MT_3 binding [18] led us to propose that MT_3 binding site is the quinone reductase 2 protein. Nevertheless, the molecular relationships between QR2 activity and the MT_3 binding site[1] are not yet well known. It is noteworthy that quinone reductase status [19,20] as well as the endogenous ligand of MT_3, i.e. MLT [21–24], have been described as participants in cellular redox processes.

The QR2 is a flavin adenine dinucleotide (FAD)-dependent homodimer that catalyses a two electrons reduction of quinone to hydroquinone by using the co-substrate dihydronicotinamide riboside (NRH) as an electron donor [25,26]. The molecular mechanism of QR2 has been compared with the well described ''ping-pong bi bi'' mechanism of action of quinone reductase 1 (QR1). Indeed, crystal structures of either enzyme reveals that they have similar catalytic sites even though they require different cofactors [27–30]. Recently, a ''ping-pong'' kinetic mechanism has been described for QR2 from human red blood cells underlying the two redox status of the FAD cofactor, leading to an oxidized and a reduced form of the enzyme. It was reported by these authors that isolating the enzyme in the different redox states was difficult if not impossible [31]. Crystallisation and co-crystallisation experiments [32] also brought information on the apparently large catalytic site of QR2, explaining the wide variety of compounds this enzyme seems to accept as substrates or inhibitors (see Vella et al. [33] for review).

[1] Since MT_3 is not a receptor (i.e. a seven transmembrane domain protein, like MT_1 or MT_2), we decided to use the term 'binding site' to qualify MT_3. Indeed, even if the actual MT_3 is a soluble enzyme, quinone reductase 2, it seems that the use of the term 'receptor' (in the sense of target protein) might lead the reader towards the notion, as in the initial literature, that MT_3 is indeed a receptor closely resembling MT_1 or MT_2.

The aim of the present study was to determine whether the MT_3 melatoninergic binding site corresponds to the catalytic site of hQR2. To test this, we developed enzymatic assays to determine the kinetics of inhibition of the specific MT_3 ligands, 2-iodo-MCA-NAT as well as 2-iodo-MLT, using excess of the co-substrate BNAH or of the substrate menadione. We generated and characterized a CHO cell line that stably express hQR2. Then, the effects of MT_3 ligands on hQR2 cellular activity led us to identify two chemical classes of compounds which can also be distinguished by their binding at the MT_3 site from brain homogenates [34]. The pharmacological properties of these compounds were compared in MT_3 binding and QR2 inhibition assays.

2. Materials and methods

2.1. Reagents and drugs

The 2-[^{125}I]-MLT radioligand (2-[^{125}I]-iodomelatonin; specific activity: 2000 Ci/mmol) was purchased from NEN (Boston, MA) whereas 2-[^{125}I]-MCA-NAT (2-[^{125}I]-iodo-5-methoxycarbonylamino-*N*-acetyltryptamine; specific activity: 2000 Ci/mmol) was custom-synthetized by Amersham Pharmacia Biotech (Orsay, France). Melatonin (MLT or *N*-acetyl-5-methoxytrytamine), 2-iodomelatonin (2-I-MLT or 2-iodo-*N*-acetyl-5-methoxytrytamine), *N*-acetyl-serotonin (NAS or *N*-acetyl-5-hydroxy-tryptamine) and menadione were obtained from Sigma (Saint Quentin Favallier, France), MCA-NAT from Tocris (Bristol, UK) and dihydrobenzylnicotamide (BNAH) obtained from Maybridge (Cornwell, England). AFMK (N^1-acetyl-N^2-formyl-5-methoxy-kynurenamine) and AMK (N^1-acetyl-5-methoxykynurenamine) were synthesized by Prof. Gérald Guillaumet (Institut de Chimie Organique et Analytique, Université d'Orléans, Orléans, France). Nineteen compounds were evaluated including bicyclic, tricyclic and tetracyclic molecules. The bicyclic molecules are compound **1**: *N*-[2-(7-methylaminosulfonyl-1-naphthyl)ethyl]acetamide, compound **8**: methyl-1-(2-acetamidoethyl)-7-naphthylcarbamate [35], compound **3**: *N*-[2-(2-phenyl-3-benzothienyl)ethyl]-3-butenamide [36], compound **4**: *N*-methyl-[4-(2,3-dihydro-1,4-benzodioxin-5-yl)]butanamide [37], compound **6**: *N*-[2-(5-methoxy-4-nitro-1*H*-indol-3-yl)ethyl]acetamide, compound **7**: *N*-[2-(5-methoxy-7-nitro-1*H*-indol-3-yl)ethyl]acetamide, compound **9**: *N*-[2-(2-iodo-5-methoxy-1-methyl-4-nitroindol-3-yl)ethyl] acetamide, [34] and compound **11**: *N*-[2-(5-methoxy-1-methyl-2-phenyl-1H-pyrrolo[3,2-b]pyridin-3-yl)ethyl]acetamide [38]. The tricyclic molecules are: compound **5**: *N*1-[2-(3-methoxy-6,7,8,9-tetrahydropyridol[3,2-*b*]indolizin-5-yl)ethyl]acetamide, compound **10**: *N*-[2-(8-methoxy-3,4-dihydro-2H-pyrido[2′,3′:4,5]pyrrolo[2,1-*b*][1,3]oxazin-10-yl)ethyl]-2-furamide and compound **32**: *N*-[2-(2-hydroxy-6,7,8,9-tetrahydropyrido[2,3-b]indolizin-10-yl)ethyl]-2-furamide [39]. The tetracyclic molecules are compound **26**: *N*1-[2-(2-methoxy-6H-pyrido[2′,3′:4,5]pyrrolo[2,1-a]isoindol-11-yl)ethyl]-acetamide, compound **27**: *N*-[2-(2-methoxy-6H-pyrido[2′,3′:4,5]-pyrollo[2,1-*a*]isoindol-11-yl)ethyl]-2-furamide, compound **28**: *N*-[2-(11-methoxy-6,7-dihydro-5H-pyrido[2′,3′:4,5]-pyrrolo[2,1-*a*][2]benzazepin-13-yl)ethyl]acetamide, compound **29**: 2-(2-methoxy-6H-pyrido[2′,3′:4,5]pyrrolo[2,1-*a*]isoindol-11-yl)ethylamine(1,6) oxalate, compound **30**: [S 28128], 2-iodo-*N*-[2-(2-methoxy-6H-pyrido [2′,3′:4,5]pyrrolo[2,1-*a*]isoindol-11-yl)ethyl]-benzamide, compound **31**: *N*-[2-(2-methoxy-6H-dipyrido[2,3-*a*:3,2-*e*]pyrrolizin-11-yl)ethyl]-2-furamide, compound **33**: *N*-[2-(2-methoxy-6-oxo-6H-pyrido [2′,3′:4,5]pyrrolo[2,1-*a*]isoindol-11-yl)ethyl]-2-furamide and compound **34**: *N*-[2-(2-methoxy-6-oxo-6H-pyrido[2′,3′:4,5]pyrrolo[2,1-*a*]isoindol-11-yl)ethyl]acetamide [39] (see some structures in Fig. 1). All compounds were dissolved in DMSO at a stock concentration of 10 mM and stored at −20 °C until experimental use.

2.2. Generation of a monoclonal anti-hQR2 antibody

Monoclonal antibodies directed against hQR2 protein were custom-made by Indicia Biotechnology (Oullins, France). Briefly, BALB/c mice were immunized with purified hQR2 (four times 50 μg: day 1, 22, 41 and 63) using Freud's adjuvant. Specific antibodies in these mice sera were tested at day 49 by specific hQR2 ELISA using a rabbit anti-peptide hQR2 antibody (see below). The animals were sacrificed at day 63. Spleen cells were then fused with Sp2/Oag-14 hybridoma cells using polyethylene glycol. Hybridoma cells were then cloned in six 96-well plates by limit dilution method. Secreting anti-hQR2 immunoglobulin clones were revealed by testing the culture supernatants by anti-hQR2 ELISA. Plates were coated with purified hQR2 (50 ng/well) for 2 h at room temperature. After washes with PBS buffer, 100 μl of hybridoma supernatants were incubated in each plate well for 2 h at room temperature. After washes of the wells using 3× 200 μl of PBS buffer per well, the revelation was performed using a goat anti-mouse anti-IgG coupled to horseradish peroxidase (ref. BI12413C, P.A.R.I.S., Compiègne, France). The HRP activity was revealed using OPD tablets (Sigma, St. Louis, MO). Thirteen clones exhibiting an $O.D._{450}$ above 0.3 unit were selected and amplified. All the clones were further characterized by western blot and immunofluorescence on naïve CHO-K1 and CHO-hQR2 cell lines. Two clones 3E6B7 and 3E6G3 were finally selected. The clone 3E6B7 supernatant was used in the present experiments.

2.3. Establishment and characterization of stable transfected cell lines

The CHO-K1/hQR2 cell line was established according to Nosjean et al. [13]. The CHO-K1/hQR2 cells maintained in Ham's F12 medium supplemented with 10% fetal calf serum, 2 mM glutamine, 500 IU/ml penicillin and 500 μg/ml streptomycin were transfected by the pcDNA3.1(+)-hQR2 plasmid using lipofectamine as described by the manufacturer (Life Technologies). Stably transfected cells were selected with neomycin (500 μg/ml). Two different clones, expressing the transgene, were grown. About 1 million cells were pelleted by centrifugation and suspended in a lysing buffer comprising: 50 mM Tris/HCl, pH 8.5, and 1 mM octyl-glucanosyl. The lysate was treated by Dounce homogenization and centrifuged. The supernatant was analysed by SDS-PAGE, Western blotting and developed using a rabbit anti-QR2 peptide (ASDITDEQKKV-READ) antibody 1/100th. After extensive washings in TBS/Tween 20 (0.1%), the blot was revealed by ECL according to Amersham® protocol.

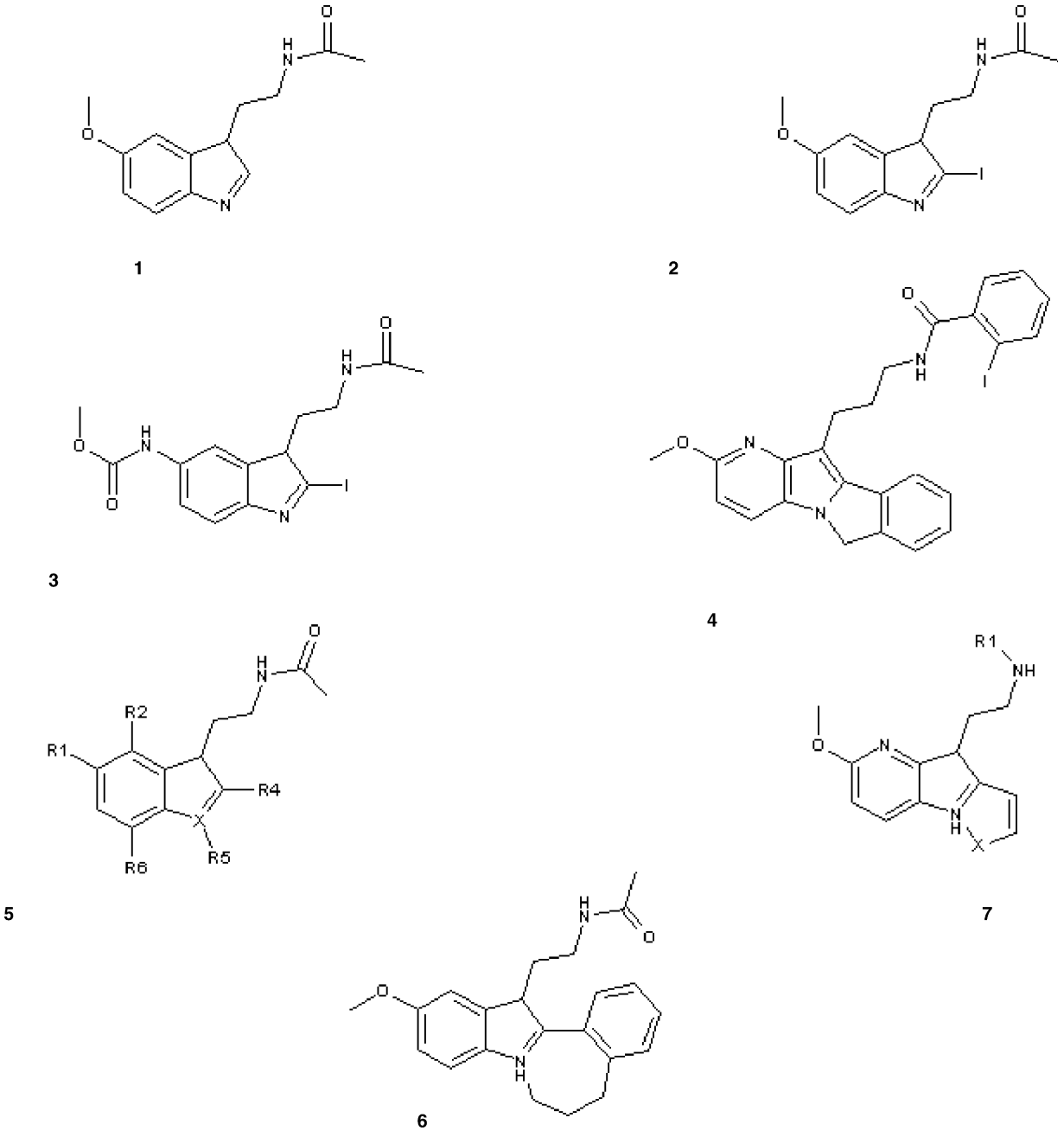

Fig. 1 – Chemical structure of the specific MT_3 compounds: reference compounds; [^{125}I]-radiolabelled compounds used for the binding studies and chemical structure of each class of compounds. (1) Melatonin; (2) 2-iodomelatonin; (3) iodo-MCA-NAT; (4) IMPPID (S 28128); (5) bicyclic inhibitors; (6) and (7) tetra- and tri-cyclic inhibitors.

2.4. QR2 immunostaining

CHO and CHO-hQR2 cell lines were cultured for 24 h on poly-D-lysine Cellware eight-well culture slide (Becton Dickinson, Franklin Lakes, USA). After 24 h, cells were fixed with 4% paraformaldehyde (Sigma, St. Louis, USA). After quenching and permeabilization steps, cells were incubated for 1 h at room temperature with the monoclonal anti-hQR2 3E6B7 antibody (dilution 1/100). After washing steps, cells were incubated with Alexa 488 labelled secondary anti-mouse Ig antibody (dilution 1/250, Molecular Probes, Invitrogen, Carlsbad, USA) for 1 h at room temperature. After final washes, slides were mounted in PermaFluor Immunon (Thermo Shandon, Runcorn, UK) and analysed by epifluorescence on an inverted Axiovert 200 microscope (Zeiss, Germany).

2.5. Biological preparations

The CHO-K1 cells stably expressing the hQR2 (CHO-hQR2) were grown to confluence, harvested in phosphate buffer containing 2 mM EDTA and centrifuged at 1000 × *g* for 5 min (4 °C). The resulting pellet was suspended in 50 mM Tris/HCl, pH 8.5, and homogenized for 1 h at 4 °C using a rotative agitator. The nuclei and cell debris were eliminated by

centrifugation (4000 × *g*, 5 min, 4 °C). Aliquots of supernatant were stored at −80 °C until use. For the sub-cellular localization characterisation experiments, the CHO-hQR2 cells were lysed and centrifuged as above, twice, at 100 000 × *g* at 4 °C. The pellets were combined, and were used as membrane-rich fractions. The supernatants were combined and used as cytosol fractions. Increasing amounts of membrane of cytosolic fractions were tested for specific binding of either 2-[^{125}I]-MLT and 2-[^{125}I]-MCA-NAT. Samples were prepared from hamster kidneys as in Nosjean et al. [13], for comparison. For CHO-hQR2 cell solubilized proteins fractions, 1 mM *n*-octyl-β-D-glucopyranoside was added in the buffer as described above for all the steps of preparation. Briefly, the pellets were homogenized for 1 h at 4 °C using a rotative agitator and were then centrifuged twice at 100 000 × *g* at 4 °C. The combined supernatants corresponds to the solubilized protein fractions. The determination of protein content was performed according to the Bradford method [40] using a Biorad kit (Bio-Rad SA, Ivry-sur-Seine, France).

2.6. 2-[^{125}I]-MLT and 2-[^{125}I]-MCA-NAT binding assays

The biological sources (typically at 500 μg/ml in 200 μl) were incubated with 2-[^{125}I]-MLT or with 2-[^{125}I]-MCA-NAT for 15 min at 4 °C in 50 mM Tris/HCl, pH 8.5, containing 1 mM *n*-octyl-β-D-glucopyranoside. In saturation assays, 2-[^{125}I]-MLT was used with concentrations ranging from 150 pM to 20 nM while concentrations of 2-[^{125}I]-MCA-NAT were from 500 pM to 7 nM according to Nosjean et al. [14]. Non-specific binding was determined with 100 μM MLT. In competitive assays, the concentrations of 2-[^{125}I]-MLT and 2-[^{125}I]-MCA-NAT were maintained between 0.75 and 0.9 nM and between 0.2 and 0.3 nM, respectively, and compounds stored in DMSO were diluted in the buffer in the range of 1 pM–1 mM (DMSO < 5% in incubation conditions). Non-specific binding was determined with 10 μM MLT [9,12,14]. All reactions were performed using a 96-well gel-filtration technique. Multiscreen 96-well filtration plates and column loader were purchased from Millipore Corp. (Bedford, MA). The Sephadex G25 superfine (Amersham Pharmacia, Piscataway, NJ) was used as a phase to separate the non-binding radioligand fraction to the radioligand bound at the solubilized proteins of CHO cells. This resin was dispensed into the 96 well, swollen with 300 μl/well of water for 4 h at 4 °C and rinsed three times with 100 μl of water by centrifugations at 1750 × *g* for 25 s at 4 °C. At the end of the incubation time, 100 μl binding mixture was loaded into individual wells in the gel filtration plate and centrifuged at 1750 × *g* for 25 s at 4 °C. Before counting the sample in the 96-well plate with a Packard Topcount microplate counter, 300 μl of MicroScint20 (Packard, Meriden, CT) was added to each well.

Data were analysed by using the program PRISM (GraphPad Software Inc., San Diego, CA). For saturation experiments, the maximal concentration of binding sites (B_{max}) and the dissociation constant of the radioligand (K_D) values were calculated according to the method of Scatchard [41]. For the competitive assay, inhibition constants (K_i) were calculated according to the Cheng–Prussof equation [42]: $K_i = IC_{50}/[1 + (L/K_D)]$, where IC_{50} is the inhibitory concentration 50% and *L* is the concentration of 2-[^{125}I]-MLT or 2-[^{125}I]-MCA-NAT.

2.7. hQR2 enzymatic activity

2.7.1. Fluorescent assay

The hQR2 enzymatic activity was measured using 100 μM menadione as substrate and 100 μM of dihydrobenzylnicotamide (BNAH) as co-substrate [13,14,18,43]. The oxydoreduction reaction was performed at 25 °C in a 200 μl of 50 mM Tris/HCl, pH 8.5, 1 mM *n*-octyl-β-D-glucopyranoside. The enzymatic kinetic measured the decrease of BNAH fluorescence corresponding to the co-substrate oxidation. This reaction was followed at 440 nm with excitation at 340 nm (Polastar 96-well plate reader, BMG, Offenburg, Germany). The slope of the decrease of BNAH fluorescence was determined using FLUOstar Optima software (BMG) and was expressed in nmol/min/mg of protein. This measure corresponds to the maximal activity of the oxidoreduction reaction. For inhibitory hQR2 enzymatic activity assay, compounds were used in the range of 1 pM–1 mM. The inhibitory concentration 50% (IC_{50}) and the inhibition percentage of BNAH oxidation of each compound were determined by using the program PRISM (GraphPad Software Inc., San Diego, CA).

Two redox states of the FAD cofactor into the hQR2 protein were studied in the presence of 100 μM substrate (oxidized form: QR2-FAD) or 100 μM co-substrate (reduced form: QR2-FAD-H_2). It is not conceivable that only the oxidized or the reduced forms of the enzyme existed at one given moment. For both redox forms of QR2, enzymatic competitive assays were performed with specific MT_3 compounds used for binding assay (2-iodo-MLT, 2-iodo-MCA-NAT) or each inhibitor belonging to the different chemical classes (bicyclic, tricyclic or tetracyclic) which were used in the range of concentrations fixed around their IC_{50}. For the oxidized or reduced forms of QR2, various concentrations of compound, respectively, competed with the range of 10–75 μM of co-substrate or substrate. The type of compound competition with BNAH or menadione was determined by Lineweaver–Burk analysis. For these competitive inhibitory assays, inhibition constants (K_i) were calculated for each type of competition according to Michaelis–Menten equation: competitive $K_i = [I]/(K_{m_{inhibitor}}/K_{m_{control}} - 1)$; uncompetitive $K_i = [I]/(K_{m_{control}}/K_{m_{inhibitor}} - 1)$ where [I] is the concentration of inhibitor and K_m is the concentration that induces only 50% of the maximal enzymatic activity. The $K_{m_{inhibitor}}$ and $K_{m_{control}}$ were analysed by using the program PRISM.

2.7.2. HPLC approach

An alternative method to measure QR2 activity was necessary whenever the tested compounds were suspected to quench the BNAH fluorescence. This alternative method was used only for five compounds (**5**, **26**, **28**, **29** and **32**). This assay has been fully described and assessed in Boutin et al. [43]. The enzymatic activity was measured in 100 μl of a 50 mM Tris/HCl pH 8.5, 1 mM *n*-octyl-β-D-glucopyranoside buffer containing 100 μM menadione and 100 μM BNAH. The QR2 activity was determined in presence of various compounds used in a range of 10 nM–100 μM. The enzymatic reaction was performed at room temperature during 12 min and stopped by the addition of 100 μL of acetonitrile. One minute prior HPLC analysis, 50 μl of TCA 20% was added to the mixture by the HPLC injector. Eighty microliters of this solution were analyzed by RP-HPLC on a

Platinum EPS C18 (Alltech, France) column (150 mm × 4.6 mm), using an Agilent 1100 series system, by means of a linear 30–85% acetonitrile gradient in 0.1% aqueous TFA over 9 min (flow rate = 1 ml/min) [43]. The assay was evaluated by analysing the reaction component stability after the assay was stopped by acetonitrile. Furthermore, the stability of these components in the HPLC mobile phase was also confirmed, since similar results were obtained with menadione, using both methods. The stability of quinones during acidic HPLC analyses have been shown in several reports (e.g. Teshima and Kondo, [44]; Suhara et al. [45]). Furthermore, BNAH seemed to be stable for a longer period of time than the classical and natural dihydronicotinamides under acidic conditions. Incubations of BNAH with QR2, in the absence of substrate, did not lead to any co-substrate consumption, suggesting again, that BNAH might be far more stable than NRH or NADH. The capacity of compounds to inhibit the enzymatic activity was established by comparing the area under curve (AUC) values of BNAH peak on the chromatograms (Fig. 2). The percentage of inhibition of hQR2 activity, induced by a compound, was calculated in reference to two AUC values of BNAH peak: the AUC value obtained in the absence of compounds, corresponding to the maximal activity (100%) of the oxidoreduction reaction; the AUC value obtained only with a substrate and co-substrate mixture corresponding to no hQR2 enzymatic activity. The inhibitory concentration 50% (IC_{50}) was determined by using the software PRISM (GraphPad Software Inc., San Diego, CA).

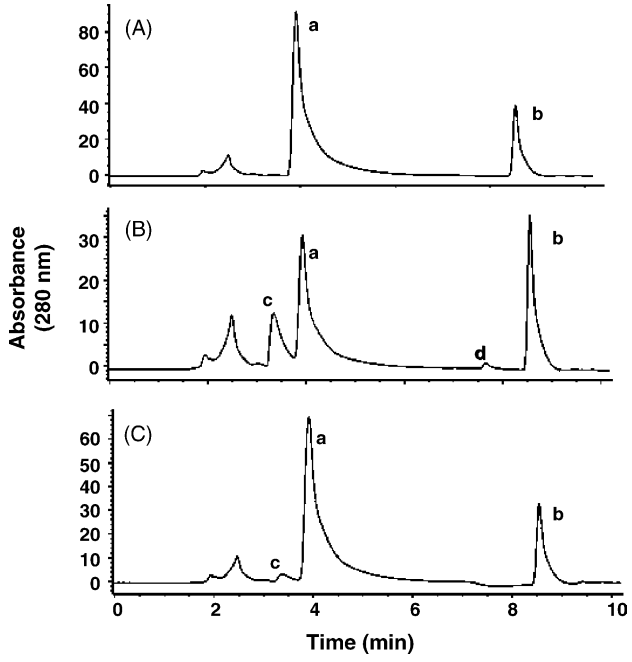

Fig. 2 – Representative chromatographic profiles of the hQR2 enzymatic reaction in absence or presence of compound 29. (A) Mixture of 100 μM BNAH and 100 μM menadione. Peaks (a) and (b) correspond to BNAH and menadione, respectively. (B) Oxidation of BNAH in BNA and reduction of menadione in menadiol by hQR2. Peaks c and d correspond to BNA and menadiol, respectively. (C) Effect of 10 μM of compound 29 on the hQR2 enzymatic activity. The enzymatic reaction was performed as described under Section 2 in presence of 100 μM BNAH and 100 μM menadione during 12 min, then stopped by the add of 100 μl acetonitrile. Just before the injection on the column, 50 μl TCA 20% was added to the mixture and 80 μl of this solution was analysed by HPLC. Platinum EPS C18 column, 150 mm × 4.6 mm; flow rate, 1 ml/min; solvent A, 0.1% TFA; solvent B, acetonitrile, 0.1% TFA. The gradient was 30–85% B in A in 9 min.

2.7.3. *Determination of the Michaelis–Menten constant (K_m): substrate and co-substrate*

The K_m values of the substrate and co-substrate were determined by both fluorescent and chromatographic techniques. For the determination of the K_m of the co-substrate, the BNAH concentrations were varied from 20 to 500 μM whereas the substrate concentration was constant [100 μM]. For the determination of the K_m of the substrate, the menadione concentrations were varied from 5 to 100 μM while the co-substrate concentration was equal to 100 μM. The experiments were repeated five times. For the treatment of the data, both Lineweaver–Burke and Eadie–Hofstee plots were used and gave similar results.

2.8. *Statistical analyses*

For the correlation analysis, the K_i values of the different chemicals for the 2-[^{125}I]-MLT or 2-[^{125}I]-MCA-NAT were expressed as pK_i corresponding to the logarithmic expression of K_i[pK_i = – log(K_i)] in order to use statistical analysis in a Gaussian distribution. To calculate the correlations between binding affinities, Pearson product-moment correlation coefficients "r" were used.

3. Results

3.1. *CHO-hQR2 cell line description*

The stable cell line was established by Nosjean et al. [13]. As shown in Fig. 3A, the use of a monoclonal anti-hQR2 antibody permitted to visualize the over-expression of the transgene in these cells (compare top and bottom panels). The signal in the control cells is barely visible. Using a polyclonal anti-hQR2 peptide antibody, Western blot analysis clearly shows the presence of the protein in two different CHO-hQR2 clones (Fig. 3B, lines A and C), while it was very faint in naïve CHO cells (Fig. 3B, line B). The QR2 activities were measured for the naïve cells, with menadione and BNAH as substrate and co-substrate respectively, at 5 ± 0.5 nmol/min/mg protein. In the transfected cells, the QR2 activity, using the same assay, was measured at 2457 ± 100 nmol/min/mg protein. In addition, the 2-[^{125}I]-MLT binding was negligible, in naïve cells (with up to 2 mg/ml of protein in the assay), when compared to specific binding in hQR2-expressing CHO cells (see Fig. 3C, top and bottom panels). Similar results were obtained whether the radioligands 2-[^{125}I]-MLT or 2-[^{125}I]-MCA-NAT were used.

3.2. *Biological material characterisation*

We began our studies by comparing QR2 activity measurements in homogenate and in cytosolic or membrane-rich

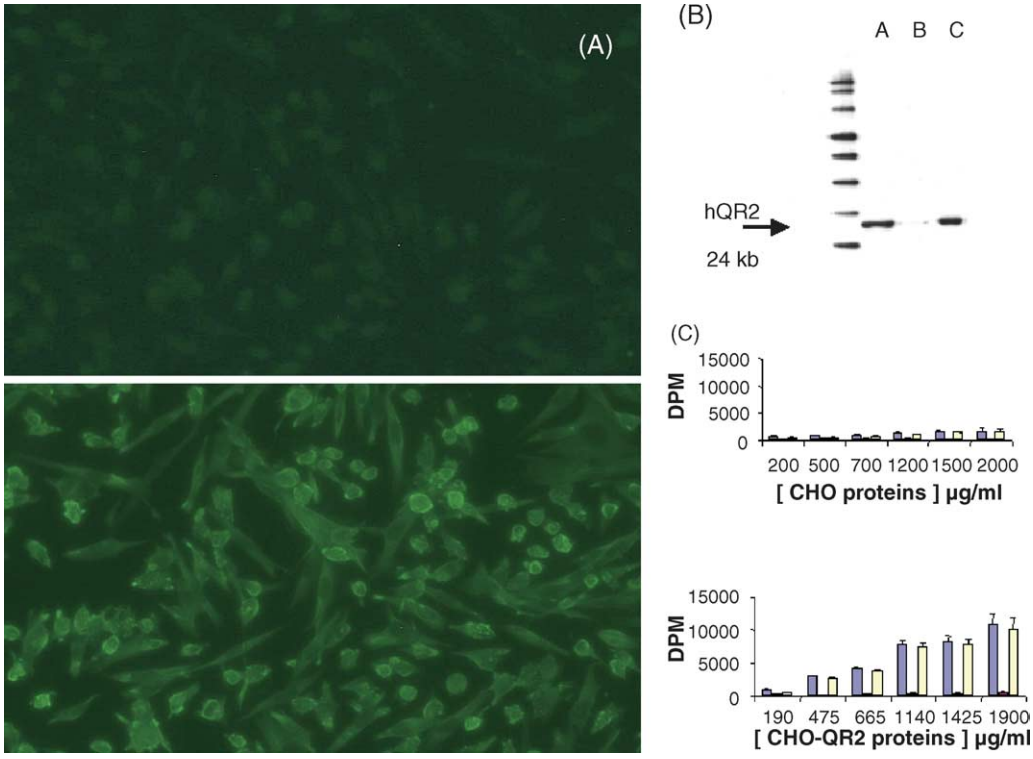

Fig. 3 – Characterization of the CHO cell line expressing the recombinant human quinone reductase 2. (A) Immunofluorescence analysis of CHO cells expressing hQR2. Naïve (top) and hQR2-transfected (bottom) cells were stained with a monoclonal anti-hQR2 antibody. Fluorescence was analysed under Axiovert 200 microscope (objective 16×). (B) Western blot analysis of two different clones of CHO stably expressing the recombinant human quinone reductase 2 using rabbit anti-QR2 polyclonal antibody directed towards the peptide ASDITDEQKKVREAD from the human sequence of QR2. Lanes (A) and (C), samples from cytosol of two different CHO-hQR2 clones. Lane (B) is from naïve CHO cells. The lane on the left side contains standard molecular weights. (C) MT_3 binding of naïve CHO cells (top) and CHO cells stably expressing the recombinant quinone reductase 2 (bottom). Using 2-[^{125}I]-MLT, classical binding experiments were performed, at increasing concentrations in cell homogenate proteins. Each point is represented by three histograms, from left to right: total, non-specific and specific bindings. The data is expressed in crude dpm. The experiments were repeated three times for the recombinant cells, and more than 20 for the naïve CHO cells. These are representative histograms obtained the same day, same experiments.

fractions. QR2 is a dimeric enzyme. Its dimerization might influence its behaviour, on one hand, and on the other, measurements of binding on a pure protein requires a large amount of protein, since specific binding only will be measured. Membranes were prepared by ultracentrifugations at 100 000 × *g*. The pellets obtained were used as membrane sources, and their capacity to bind the ligands was evaluate in comparison with the supernatants of these same preparations (i.e. the cytosol) and with the homogenates. The results are summarized in Fig. 4. On the left panels, the binding of 2-[^{125}I]-MLT to either homogenate (A), membrane (B) or cytosol fractions (C) from CHO-hQR2 cells are presented, while on the right ones, the binding from the same fractions from hamster kidneys are shown (D, E and F, respectively). Similar results have been obtained when 2-[^{125}I]-MCA-NAT was used as a specific MT_3 ligand (not shown). There was approximately 10 times more binding signal in CHO-QR2 than in hamster kidneys. 2-[^{125}I]-MLT binding could not be detected in naïve CHO cells [5,13]. In samples from fractionated cells, all the binding signal was found in cytosol of CHO-QR2. In hamster kidneys, a small portion of the signal was associated with the plasma membranes (less than 10%). Indeed, when membranes from hamster kidneys were intensively washed, the same portion of binding remains associated with the membrane fraction. Scatchard analyses on fractions from hamster kidney membranes and cytosol as well as on CHO-QR2 cytosol revealed 2-[^{125}I]-MLT K_D's of 1.4, 13 and 4 nM, respectively (Fig. 5). Furthermore, the use of a mild detergent in the preparation of the cytosol, by treating homogenates with *n*-octyl-β-D-glucopyranoside did not change the behaviour of the binding site (not shown) nor did it change the QR2 catalytic activity.

3.3. *Saturation assay*

Saturation studies using 2-[^{125}I]-MLT ($n = 2$) or 2-[^{125}I]-MCA-NAT ($n = 2$) revealed a single binding site in CHO-hQR2 cell line (Fig. 6). The concentration of 2-[^{125}I]-MLT binding sites (B_{max}) was 1000 ± 75 fmol/mg protein and 139 ± 21 fmol/mg for the 2-[^{125}I]-MCA-NAT ones. The K_D of 2-[^{125}I]-MLT in CHO-hQR2 preparations was 4.4 ± 0.4 nM and 0.47 ± 0.02 nM for 2-[^{125}I]-MCA-NAT. These figures compare well with B_{max}'s measured in hamster kidneys (89 fmol/mg Prot [9] or 173 fmol/mg Prot

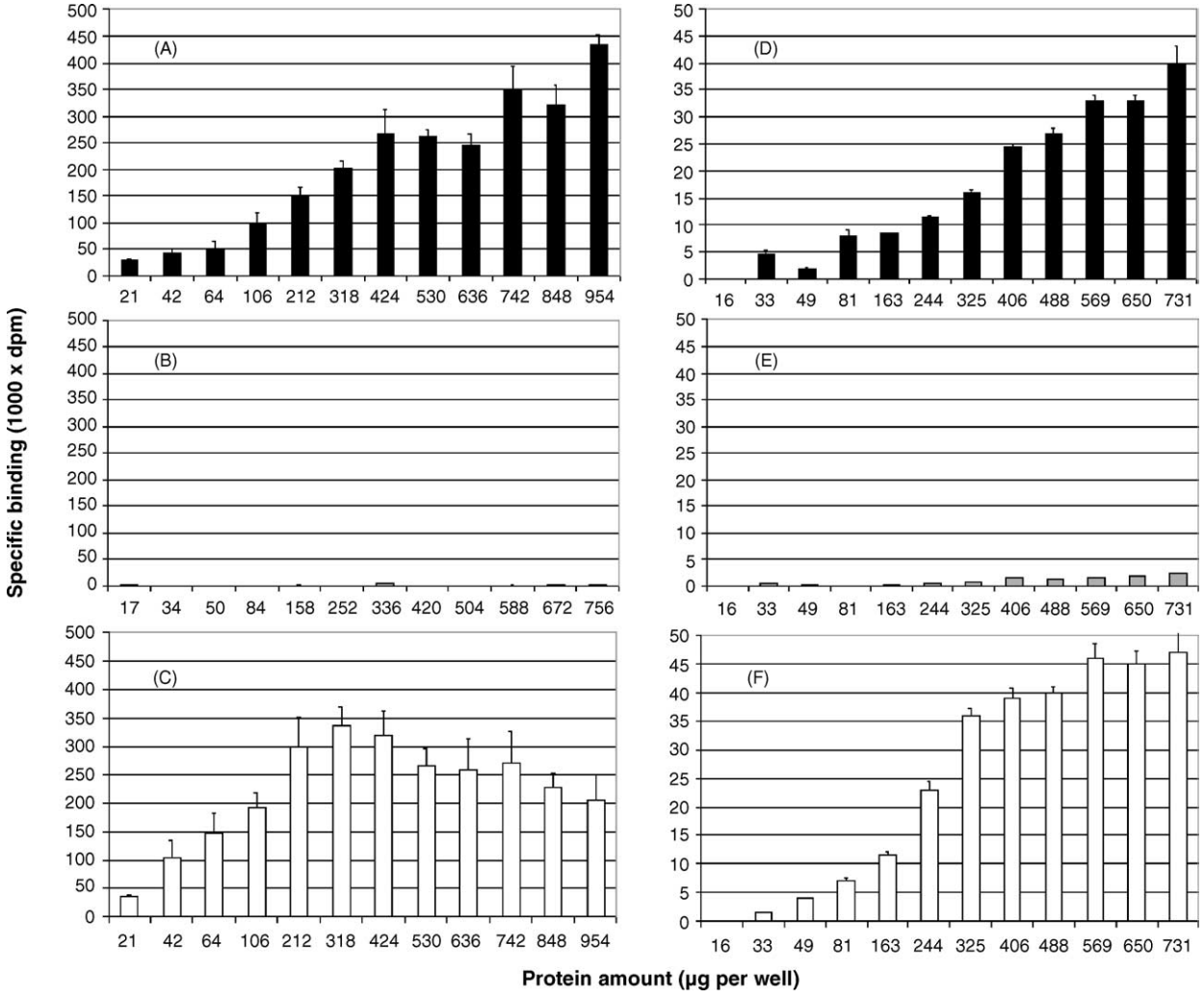

Fig. 4 – Comparison of the sub-cellular localization of 2-[^{125}I]-MLT binding in CHO-hQR2 cells and in hamster kidneys. Increasing amounts of proteins (from 16 to 954 μg) from homogenate (A), membrane-rich fractions (B) and cytosol (C) of CHO-hQR2 cells or of Hamster kidneys (D–F) were incubated with 2-[^{125}I]-MLT. Data are presented as means of 3 measurements, and are representative of 3 independent experiments. Note that the binding in membranes from hamster kidneys (E) is low but can be measured, while in membrane from CHO-hQR2 (B), the binding is barely detectable. Note the 10-fold difference between the recombinant cell data (left panel) and the hamster tissues data (right panels).

[14]). These B_{max}'s are 5–10 times higher than those measured in hamster brain (19.7 fmol/mg Prot [12]).

3.4. *Competitive assay on 2-[^{125}I]-MLT and 2-[^{125}I]-MCA-NAT binding*

A correlation analysis of the K_i values for each compound (except for compound **4**) determined from both 2-[^{125}I]-MLT and 2-[^{125}I]-MCA-NAT competitive binding assays was established to compare the pharmacological properties of each compound at both binding sites (Tables 1 and 2). There is a highly significant correlation between 2-[^{125}I]-MLT and 2-[^{125}I]-MCA-NAT binding profiles on homogenates from hQR2-expressing CHO cells [$r = 0.82$, $p < 0.0001$, $n = 28$, Fig. 7, Table 2]. Analysis of reference compounds also showed a high correlation [$r = 0.81$, $p < 0.005$, $n = 9$, Table 2], as well as for the tri- or tetracyclic ones [$r = 0.85$, $p < 0.001$, $n = 10$, Table 2]. To the contrary, there was no correlation for the bicyclic molecules [$r = 0.66$, $p > 0.05$, $n = 9$, Table 2] and only compound **4** at 100 μM was not active on the 2-[^{125}I]-MLT binding competition assay whereas it could fully inhibit the 2-[^{125}I]-MCA-NAT binding (Table 1).

3.5. *Determination of K_m for hQR2 enzymatic activity*

The Michaelis constants (K_m) of hQR2 for its substrate, menadione, and co-substrate, BNAH, were determined using two differencent assays. For menadione, the K_m's were in the same range with both assays: 6.7 ± 1.6 μM for enzymatic fluorescence assay and 17 ± 4 μM for the HPLC approach. Conversely, similar results were observed for the BNAH: $K_m = 20 \pm 6$ μM when determined by enzymatic fluorescence assay or 40 ± 8 μM for the HPLC approach. BNAH, when compared to other hydrure donors is exceptionally stable in

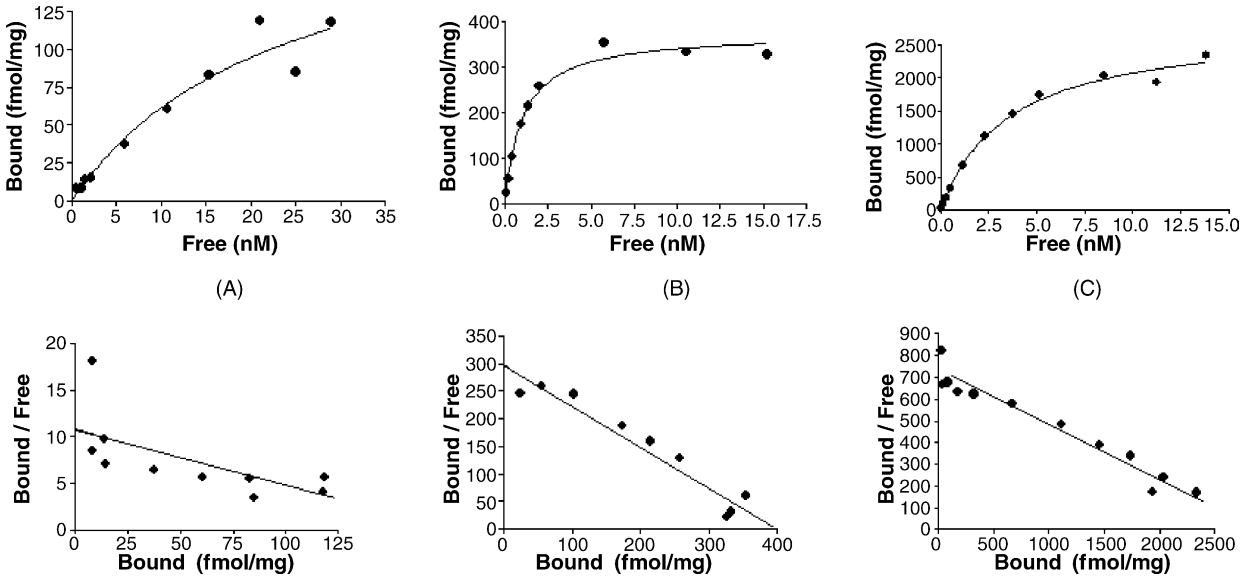

Fig. 5 – Scatchard plots of MT_3 binding in hamster kidney membranes (A) and cytosol (B) and in CHO-hQR2 cell cytosol (C). The biological samples were prepared as described in Section 2, and used to measure the binding of 2-[^{125}I]-MLT while increasing its concentration, from 0 to 20 nM at a concentration of ~500 μg/ml. Hamster kidney membranes (A) and cytosol (B) were obtained by differential ultracentrifugation as was the CHO-hQR2 cytosol sample (C).

solution. Indeed, if incubated alone with the enzyme – i.e. without substrate, but under aerobic conditions – the compound is stable for over 1 h [43].

3.6. *Comparison of melatoninergic binding versus hQR2 enzymatic inhibition*

The IC_{50} and K_i values were determined for hQR2 enzymatic and binding assays (using both 2-[^{125}I]-MLT and 2-[^{125}I]-MCA-NAT bindings) for each compound (Table 1). For hQR2 catalytic assay, most of the IC_{50} were determined using the enzymatic fluorescent assay except for several compounds (**5**, **26**, **28**, **29** and **32**) quenching the fluorescence of BNAH and for which IC_{50} were measured using the HPLC assay. These data were compared and a correlation coefficient determined as shown in Fig. 8. Amongst these results, it is noteworthy to point out the inhibition potency on hQR2 of the compound **31**, with an IC_{50} of 14 nM. Compounds **3–5**, **11**, **28**, **32–34** were inactive on the hQR2 enzymatic activity at least at concentrations below 100 μM. In addition, compound **4** was not active in the 2-[^{125}I]-MLT binding competition assay. A correlative analysis was made for the few compounds (namely, compounds **6**, **9**, **26**, **27**, **29** and **31**) that could inhibit both the hQR2 enzymatic activity and 2-[^{125}I]-MLT or 2-[^{125}I]-MCA-NAT binding. Correlations between hQR2 enzymatic activity and 2-[^{125}I]-MCA-NAT binding were different between chemical classes (Fig. 8). Thus, this correlation was significant for bicyclic molecules [$r = 0.82$, $p < 0.05$, $n = 6$, Table 2] while, by contrast, no significant correlation was observed for references [$p = 0.1$, $n = 5$, Table 2] as for the tri- or tetracyclic molecules [$p = 0.79$, $n = 5$, Table 2] (Fig. 8). The comparison between IC_{50} from hQR2 activity and K_i from 2-[^{125}I]-MLT binding values showed a significant correlation for

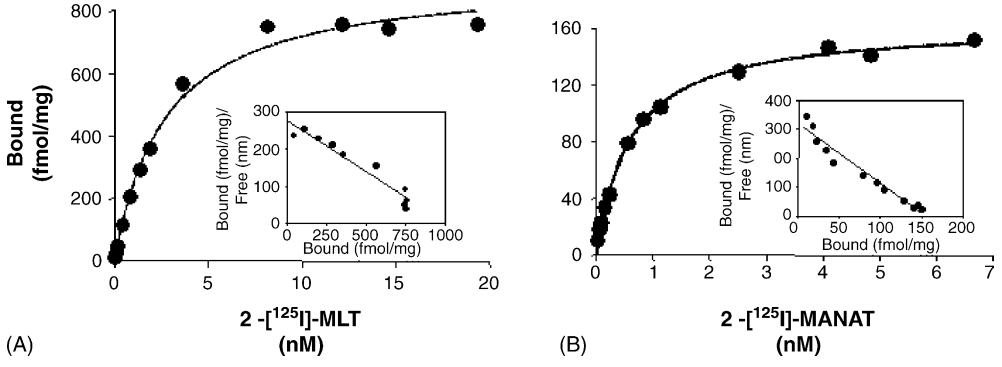

Fig. 6 – Saturation curves and Scatchard plots of 2-[^{125}I]-MLT (A) and 2-[^{125}I]-MCA-NAT (B) specific binding at the solubilized proteins expressed in CHO-hQR2 cells. The non-specific binding was determined in the presence of 100 μM of MLT. Points shown are from two representative experiments performed in quadriplicates. These plots were obtained using proteins from CHO-hQR2 cells.

Table 1 – Comparison between equilibrium binding constants (K_i) determined by competitive inhibition of 2-[^{125}I]-iodomelatonin or 2-[^{125}I]-MCA-NAT binding and inhibitory concentration 50% (IC_{50}) by inhibition assay of hQR2 enzymatic activity

Molecules	Binding 2-[^{125}I]-MLT, K_i (nM)	Binding 2-[^{125}I]-MCA-NAT, K_i (nM)	hQR2 activity assay, IC_{50} (μM)
MLT	2070 ± 470	61.0 ± 13.9	130 ± 35
MCA-NAT	940 ± 110	12.8 ± 3.8	295 ± 19
NAS	710 ± 160	31.4 ± 10.4	99 ± 14
2-IMLT	21.1 ± 8	5.1 ± 1.0	16 ± 2
BNAH	1400 ± 120	640 ± 530	ND
Menadione	20000 ± 5000	10907 ± 1350	ND
Dicumarol	55500 ± 4300	474 ± 189	590 ± 100
Prazosin	500 ± 60	304 ± 69	ND
AFMK	80000 ± 6300	6480 ± 827	ND
AMK	9800 ± 590	2422 ± 20	ND
Compound **1**	380 ± 200	73 ± 15	38 ± 5
Compound **3**	700 ± 140	138 ± 30	>10
Compound **4**	>100 μM	17610 ± 300	>10
Compound **5**	8600 ± 150	5200 ± 170	>10[a]
Compound **6**	29 ± 5	27 ± 2	1.5 ± 0.1
Compound **7**	310 ± 60	850 ± 100	44 ± 9
Compound **8**	140 ± 25	21 ± 0.1	15 ± 0.2
Compound **9**	0.5 ± 0.1	2.4 ± 0.6	0.3 ± 0.02
Compound **10**	50 ± 14	29 ± 6	5 ± 0.7
Compound **11**	940 ± 40	13.4 ± 6	>10
Compound **26**	1.7 ± 0.7	0.6 ± 0.2	1.9 ± 0.1[a]
Compound **27**	85 ± 8	5.2 ± 0.5	0.2 ± 0.07
Compound **28**	847 ± 140	270 ± 110	>10[a]
Compound **29**	13.1 ± 4.2	4.3 ± 0.8	0.87 ± 0.08[a]
S28128	54 ± 20	130 ± 40	0.91 ± 0.04
Compound **31**	5.1 ± 3.5	8.6 ± 2	0.014 ± 0.001
Compound **32**	3300 ± 190	79 ± 3	>10[a]
Compound **33**	210 ± 50	12.5 ± 3.8	>10
Compound **34**	350 ± 110	154 ± 9	>10

Inhibition constant K_i values were calculated from IC_{50} obtained from competition curves by the method of Cheng and Prussof [42]. Results are expressed by mean ± S.E.M.
[a] IC_{50} determined by HPLC approach; ND: not determined.

bicyclic molecules [$r = 0.96$, $p < 0.002$, $n = 6$, Table 2] and for references molecules [$r = 0.93$, $p < 0.03$, $n = 5$, Table 2] whereas no correlation was observed for the tri- or tetracyclic molecules [$p = 0.98$, $n = 5$, Table 2].

3.7. *Enzyme inhibition types*

The cold analogues of the MT_3 radioligands were studied to determine their inhibition type on hQR2 activity. 2-Iodo-MCA-

Table 2 – Correlation parameters between binding with different ligands and enzymatic inhibition potency

Total	References	Bicyclic	Tri- and tetracyclic compounds
Binding 2-[^{125}I]-MLT vs. binding 2-[^{125}I]-MCA-NAT			
r 0.82	0.81	0.66	0.85
p <0.0001 ***	0.0044 **	0.0769 NS	0.0009 ***
Binding 2-[^{125}I]-MLT vs. hQR2 enzymatic activity			
r 0.81	0.93	0.96	–
p 0.0001 ***	0.0237 *	0.002 **	0.9841 NS
Binding 2-[^{125}I]-MCA-NAT vs. hQR2 enzymatic activity			
r 0.54	–	0.82	–
p 0.0267 *	0.1310 NS	0.0443 *	0.7892 NS

The constants were determined for each compounds in competitive binding with 2-[^{125}I]-iodomelatonin. 2-[^{125}I]-MCA-NAT and in inhibition assay of hQR2 enzymatic activity; NS: non-significant.
* $p < 0.05$.
** $p < 0.001$.
*** $p < 0.0001$.

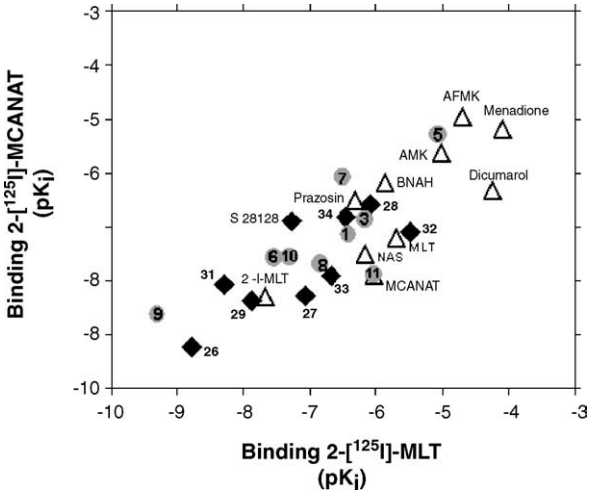

Fig. 7 – Correlation between logarithmic expression of equilibrium inhibition constants (pK_i) of reference molecules including BNAH and menadione (△), bicyclic compounds (○), tri- and tetracyclic compounds (◆), for 2-[^{125}I]-MLT and 2-[^{125}I]-MCA-NAT binding to hQR2 expressed in CHO cells. Inhibition constant K_i values were calculated by the method of Cheng–Prussof equation [40] from the inhibitory concentration 50% (IC_{50}) values obtained by using the program PRISM (GraphPad Software) in competition experiments. Points shown are mean from experiments performed in duplicates and repeated at least two times for each radioligand. The numbers refer to the compounds listed in Table 1 and described in Section 2.

NAT and 2-iodo-MLT are competitive inhibitors with BNAH at hQR2. The K_i values were estimated at 12.4 ± 2.9 μM for 2-iodo-MCA-NAT and at 50 ± 20 μM for 2-iodo-MLT, respectively (Table 3). Conversely, those two compounds were uncompetitive with menadione. The K_i values were measured at 33 ± 16 μM for 2-iodo-MCA-NAT and at 4 ± 2 μM for 2-iodo-MLT (Table 3). Another possible candidate as a ligand, the iodo derivative S28128, was uncompetitive with BNAH as well as with menadione. The Ki values were 0.18 ± 0.02 and 0.94 ± 0.24 μM, respectively (Table 3 and Fig. 9).

Among the compounds belonging to the different chemical classes, only the most potent enzymatic inhibitors of each class had been studied in the hQR2 competitive assay. Compounds **9** and **31** acted as competitive inhibitors of BNAH whereas MLT and compound **15** exerted a non-competitive mixed type inhibition with the co-substrate (Table 3). All compounds were uncompetitive with menadione (Table 3 and Fig. 9).

4. Discussion

MT_3 is the low affinity binding site of MLT that was firstly characterized using the 2-[^{125}I]-MLT ligand [11]. Later, Molinari et al. [12] have developed a new radioligand, 2-[^{125}I]-MCA-NAT, more specific for MT_3 than for the two other well-characterized MLT receptors (i.e. MT_1 and MT_2). Recently, MT_3 has been identified by resin affinity chromatography as the human oxidoreductase QR2 protein and further mass spectrometry sequencing [13]. These results have been confirmed by the absence of 2-[^{125}I]-MCA-NAT binding in the tissues (brain and kidneys) of mouse strain depleted of the QR2 gene [18]. Further information should be gathered to explain the subcellular localization of QR2. Indeed, since the original, detailed work of Duncan et al. [6], the subcellular localization of MT_3 was reported as membrane-associated. QR2 is mainly cytosolic, although it possesses a cryptic myristoylation-specific site [47]. This cryptic site can be revealed by digestion by caspase enzymes as it has been reported for the protein bid [48]. If myristoylation, a membrane-targeting event [49], can occur, it

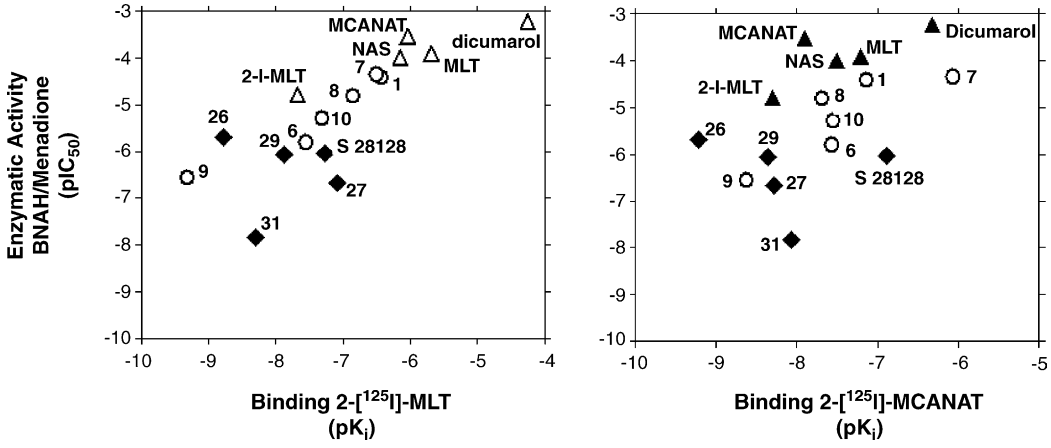

Fig. 8 – Plots of logarithmic expression of equilibrium inhibition constants (pK_i) and inhibition potencies (pIC_{50}) of compounds, respectively, determined from binding and enzymatic assays from hQR2-expressing CHO cells. Molecules were: reference compounds (△), bicyclic molecules (○), tri- or tetracyclic molecules (◆). Close symbols referred to non-significant correlations ($p > 0.05$) while the open ones showed significant correlations ($p < 0.05$). For binding and enzymatic assays, IC_{50} values were obtained by using the program PRISM (GraphPad Software) in competition experiments. For binding assay, K_i values were calculated from IC_{50} by the method of Cheng–Prussof equation [42]. Points shown are mean from experiments performed in duplicates and repeated at least two times for binding and enzymatic assays. The numbers refer to the compounds listed in Table 1 and described in Section 2.

Table 3 – Steady-state inhibition parameters of hQR2 inhibition

	Oxidized form hQR2-FAD	K_i (μM)	Reduced form hQR2-$FADH_2$	K_i (μM)
2-Iodo-MLT	Competitive	50 ± 20	Uncompetitive	4 ± 2
2-Iodo-MCA-NAT	Competitive	12 ± 3	Uncompetitive	33 ± 16
S28128	Uncompetitive	0.18 ± 0.02	Uncompetitive	0.9 ± 0.2
Melatonin	Non-competitive mixed type	ND	Uncompetitive	150 ± 20
Compound **9**	Competitive	0.08 ± 0.01	Uncompetitive	0.31 ± 0.07
Compound **31**	Competitive	0.04 ± 0.01	Uncompetitive	0.03 ± 0.01

Compounds used as radiolabelled ligands for binding assays and the most potent enzymatic inhibitor of both chemical classes were tested in full range concentrations. The two redox states of the FAD cofactor into hQR2 protein were studied in the presence of substrate (oxidized form: hQR2-FAD) or co-substrate (reduced form: hQR2-FAD-H_2) excess. For the oxidized and reduced forms of hQR2, competitions of compound were respectively measured with various concentrations of co-substrate and substrate. Results are expressed by mean ± S.D.; ND: no determined.

is possible that QR2 is directed to membranes as can be seen for NADH-cytochrome b5 reductase [50].

The aim of the present work was to characterize the MT_3 binding site at hQR2 protein and to report new molecular tools for the study of the pharmacology of MT_3/hQR2 (see review in [46]). Our data show that, in hamster kidneys, as in QR2-overexpressing CHO cells, MLT binding sites are mainly cytosolic, whereas membranes from both sources are minimally showing such binding capacities, either with 2-[^{125}I]-MLT or with 2-[^{125}I]-MCA-NAT. It has been suggested that this binding site was different from the cytosolic one, but since the binding at both localizations disappeared in tissues from QR2-deleted mice, it rather seems that QR2 is distributed at both subcellular localisations. In naïve CHO cells – as in most of cell lines – QR2 activity is low. While the measurement of its activity is easily detected in the cytosol, the activity associated with the membrane fraction of these naïve CHO cells is barely detectable with the currently available technology as also shown by Nosjean et al. [13]. In QR2-overexpressing cells, the membrane-bound QR2 specific activity is about a tenth of the cytosolic one. For the binding values, either with 2-[^{125}I]-MLT or with 2-[^{125}I]-MCA-NAT, the ratios are similar. Nevertheless, the activity is measurable enough to ensure that its pharmacology is the same than the cytosolic one (same enzymatic characteristics and same sensitivity to reference inhibitors). Further experiments are currently on their way in our laboratory to specifically address this question.

Although MT_3 has been identified as the hQR2 [13,18], the molecular relationships between QR2 activity and the MT_3 binding site are not yet well understood [13,14]. Therefore, we

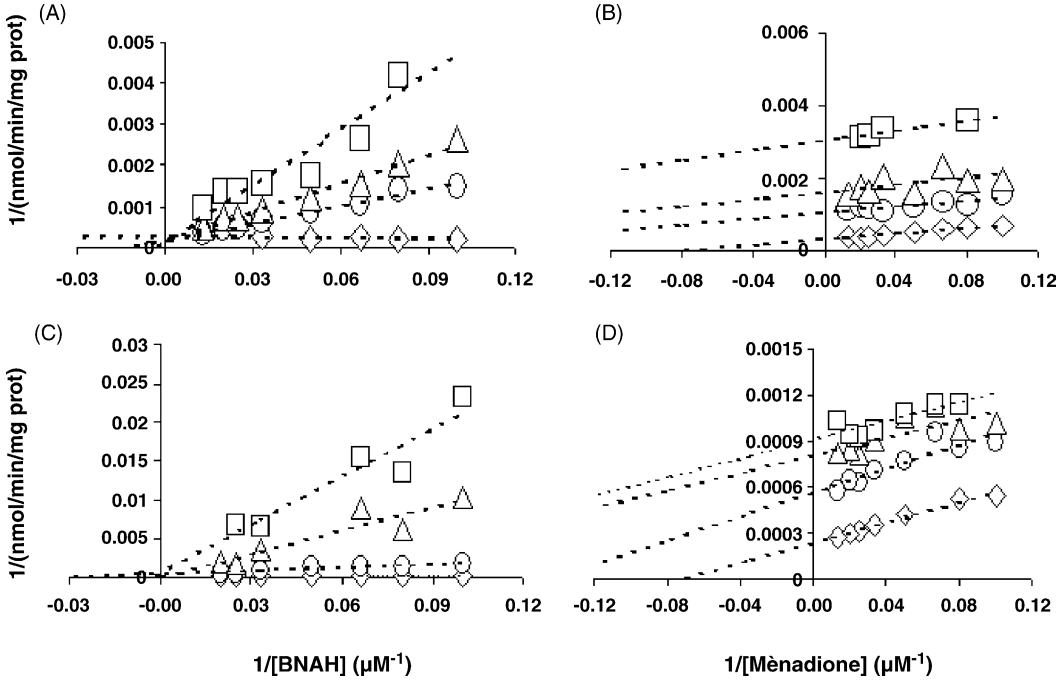

Fig. 9 – Steady-state inhibition of hQR2 by compounds used as radiobabelled ligands for binding assay as a function of the substrate or co-substrate concentration. Panels (A) and (C) have 100 μM of menadione (oxidized form of hQR2) and various concentration of BNAH (10–75 μM) while (B) and (D) panels have 100 μM of BNAH (reduced form of hQR2) and various concentration of menadione (10–75 μM). Lineweaver–Burk plot of hQR2 activity with (A) and (B): 0 μM (◇), 20 μM (○), 40 μM (△) and 100 μM (□) 2-iodo-MCA-NAT; (C) and (D): 0 μM (◇), 10 μM (○), 20 μM (△) and 50 μM (□) 2-iodo-MLT. Representative curves are shown in which each point is the mean of duplicate determinations. Similar results were obtained on at least two independent experiments.

wanted to fully characterize it using a recombinant hQR2 protein stably expressed in CHO cells. Saturation of 2-[^{125}I]-MLT or 2-[^{125}I]-MCA-NAT binding assays and Scatchard analyses revealed that recombinant hQR2 protein binding sites were saturable with a dissociation constant in the nanomolar (4.4 ± 0.4 nM) or picomolar (475 ± 20 pM) ranges, respectively. These values were similar to those previously published for MT_3 characterization from brain, kidneys and liver [11,12,14]. According to the fact that the MT_3 binding site and QR2 enzymatic activity are likely the same protein [18], our results showed that the use of CHO cell lines stably expressing hQR2 protein constitutes a valuable tool for studying the MT_3 pharmacology at hQR2 using either the melatoninergic ligand 2-[^{125}I]-MLT or a more specific one, such as 2-[^{125}I]-MCA-NAT. Actually, most pharmacological MT_3 studies were performed with compounds derived from the MLT chemical structure on homogenates of brain hamster while other reference compounds are not specific, such as prazosin and cibacron blue [6,7,9,12,14]. Therefore, in the present study, molecules belonging to two new chemical classes have been studied in hQR2-expressing CHO cells: bicyclic compounds also derived from MLT bioisosters [34] and tri- and tetracyclic compounds which have been characterized as MT_3 ligands on hamster brain homogenates using 2-[^{125}I]-MLT as radioligand (J.A. Boutin, P. Delagrange, unpublished data). Those MT_3 compounds showed similar affinities in both 2-[^{125}I]-MLT and 2-[^{125}I]-MCA-NAT competitive binding assays with a correlation coefficient of 0.82 ($p < 0.0001$). Our results from hQR2 were therefore in accordance with those of Molinari et al. [12] which showed a high correlation between 2-[^{125}I]-MCA-NAT and 2-[^{125}I]-MLT for MLT derived compounds at MT_3 binding site naturally present in Siberian hamster brain ($r = 0.962$; $p < 0.001$), although the correlation was weaker in the present case. Moreover, when the data are analysed according to the chemical classes, there was no correlation for the bicyclic compounds. In fact it is interesting to compare the K_D for both bicyclic radioligands on hamster brain and hQR2 when they have been determined in the same study. Both radioligands had similar K_D on hamster brain (390 pM for 2-[^{125}I]-MLT and 116 pM for 2-[^{125}I]-MCA-NAT, ratio 3.3 [12]) whereas on hQR2, 2-[^{125}I]-MCA-NAT was more potent (475 pM for 2-[^{125}I]-MCA-NAT and 4400 pM 2-[^{125}I]-MLT, ratio 9.3). Different technical factors, i.e. solubilized proteins, could explain these differences from transfected cells versus brain homogenate membranes. As stated above, MT_3 binding or QR2 activity could also be detected on membrane preparations but at a far lower level. The membrane or cytosolic localization of the QR2 protein may induce conformational changes of the binding site. Species differences may affect the MT_3 binding site.

The fact that two redox forms are theoretically associated with the ''ping-pong bi bi'' oxidoreductase mechanism of hQR2 [30,31] had also to be taken into consideration. This is why we attempted to favour the formation of each redox forms in the presence of an excess of either its substrate (oxidized form: hQR2-FAD) or its co-substrate (reduced form: hQR2-$FADH_2$). Unfortunately, the existence of one of the (reduced or oxidized) states seem to be barely measurable as a function of time on one hand, and on the other, the outstanding stability of BNAH [43] in incubation seemed to underline the difficulty to study these intermediary states. Furthermore, Kwiek et al. [31], showed that oxydo-reduction of the enzyme occurred in microsecond time frames, a feature incompatible with our experimental conditions. Nevertheless, our inhibition experiments of hQR2 by 2-iodo-MLT and 2-iodo-MCA-NAT revealed that both specific MT_3 ligands were antagonists, independently of the presumed redox status of hQR2 protein. Namely, they bind to the co-substrate binding site in a competitive inhibition manner, suggesting that the melatoninergic binding site corresponds to the catalytic site. Conversely, 2-iodo-MLT and 2-iodo-MCA-NAT present an uncompetitive inhibition type with the substrate at QR2 protein form, suggesting an exclusive binding to the protein–substrate complex. The MT_3 binding site might depend on the redox status of the hQR2 cofactor FAD. Conversely, different inhibition types could be observed at hQR2-FAD as, for instance with MLT, the bicyclic compound **9** and with the tetracyclic ones **30** (S 28128) and **31**, as was reported for the QR2 inhibitors: the antimalarian drugs chloroquine, primaquine and quinacrine [31]. A co-crystallisation of QR2-FAD or QR2-$FADH_2$ with bicyclic or tetracyclic compounds could be necessary to better understand these differences, as this approach has been reported for resveratrol [32].

The pharmacological properties of the different specific MT_3 compounds were studied on the QR2 protein to establish the relationship between the MT_3 binding site and the hQR2 catalytic activity. The affinities of all compounds from 2-[^{125}I]-MCA-NAT and 2-[^{125}I]-MLT competitive binding assays were compared with their IC_{50} values determined in the hQR2 activity assay. A significant correlation was observed between hQR2 activity and MT_3 binding only for compounds belonging to the bicyclic chemical family of compounds (i.e. the MLT-related chemicals). Nevertheless, those compounds were about 10–100-fold less potent in inhibiting the hQR2 enzymatic activity than in competing with 2-[^{125}I]-MCA-NAT or 2-[^{125}I]-MLT binding. These differences between the affinity and the inhibition constants may be due to the very high concentration (100 μM) of the co-substrate BNAH used in the assay. Indeed, BNAH is also a MT_3 ligand ($K_i = 640$ nM for 2-[^{125}I]-MCA-NAT). Therefore, at 100 μM, it should saturate all the MT_3 binding sites and compounds must displace BNAH from the MT_3 binding pocket in order to bind to the site and to modulate the activity of QR2. The fact that the best inhibitor (compound **31**) is also the most potent ligand is in favour of this hypothesis. By contrast, no significant correlation was observed between hQR2 activity and MT_3 binding for the tetracyclic compounds despite compound **31** being a nanomolar inhibitor of QR2 activity as well as of 2-[^{125}I]-MCA-NAT or 2-[^{125}I]-MLT binding. According to the crystal structure of QR2 [30], it is possible that the two binding sites were independent and located into the well-described large catalytic pocket. One would be responsible for the inhibition of hQR2 activity and the other for the inhibition of 2-[^{125}I]-MCA-NAT or 2-[^{125}I]-MLT binding. In favour to this hypothesis, some potent MT_3 ligands from the tetracyclic chemical classes (see Table 1: compounds **28**, **32–34**) could not inhibit QR2 activity. In a similar manner, an inhibition of the 2-[^{125}I]-MCA-NAT binding at hQR2 expressed in CHO cells was observed for estradiol ($K_i = 3$ μM) whereas this tetracyclic compound could not inhibit the hQR2 enzymatic activity [13].

In our study, we have identified compounds which are potent QR2 inhibitors. For example, compound **9** could inhibit the hQR2 activity in the same manner than 2-iodo-MCA-NAT and 2-iodo-MLT. This melatoninergic compound binds at the MT_3 binding site for the oxidized form of QR2 and impairs the electron transfer from the co-substrate to the QR2-FAD protein. Also, this new potent compound inhibits the enzymatic mechanism of QR2 through the MT_3 binding site at the first step of enzymatic reaction. Considering MT_3 as a feature of hQR2 in a particular state (i.e. oxidized) will help in the study of this membrane-bound MLT binding site in various physiopathological situations. The new molecular tools described here will also facilitate the description and comprehension of MT_3.

Acknowledgments

The authors gratefully acknowledge Lisa Maiofiss-Dullin for help in the statistical analysis of data and Dr. Roy Golsteyn to his help with the manuscript.

REFERENCES

[1] Arendt. J Melatonin Clin Endocrinol 1988;29:205–29.
[2] Delagrange P, Atkinson J, Boutin JA, Casteilla L, Lesieur D, Misslin R, et al. Therapeutic perspectives for melatonin agonists and antagonists. J Neuroendocrinol 2003;15:442–8.
[3] Dubocovich ML, Cardinali DP, Delagrange P, Krause DN, Strosberg D, Sugden D, et al. Melatonin receptors. The IUPHAR compendium of receptor characterization and classification. London: IUPHAR Media, 2000. p. 270–7.
[4] Duncan MJ, Takahashi JS, Dubocovich ML. 2-[^{125}I]iodomelatonin binding sites in hamster brain membranes: pharmacological characteristics and regional distribution. Endocrinology 1988;122:1825–33.
[5] Mailliet F, Audinot V, Malpaux B, Delagrange P, Migaud M, Barrett P, et al. Molecular pharmacology of ovine melatonin receptor: comparison with recombinant human MT1 and MT2. Biochem Pharmacol 2004;67:667–77.
[6] Duncan MJ, Takahashi JS, Dubocovich ML. 2-[^{125}I]iodomelatonin binding sites in hamster brain membranes: pharmacological characteristics and regional distribution. Endocrinology 1988;122:1825–33.
[7] Duncan MJ, Takahashi JS, Dubocovich ML. Characteristics and autoradiographic localization of 2-[^{125}I]iodomelatonin binding sites in Djungarian hamster brain. Endocrinology 1989;125:1011–8.
[8] Pickering DS, Niles LP. Pharmacological characterization of melatonin binding sites in Syrian hamster hypothalamus. Eur J Pharmacol 1990;175:71–7.
[9] Paul P, Lahaye C, Delagrange P, Nicolas JP, Canet E, Boutin JA. Characterization of 2-[^{125}I]iodomelatonin binding sites in Syrian hamster peripheral organs. J Pharmacol Exp Ther 1999;290:334–40.
[10] Dubocovich ML. Pharmacology and function of melatonin receptors. FASEB J 1988;2:2765–73.
[11] Dubocovich ML. Melatonin receptors: are there multiple subtypes? Trends Pharmacol Sci 1995;16:50–6.
[12] Molinari EJ, North PC, Dubocovich ML. 2-[^{125}I]iodo-5-methoxycarbonylamino-*N*-acetyltryptamine: a selective radioligand for the characterization of melatonin ML2 binding sites. Eur J Pharmacol 1996;301:159–68.
[13] Nosjean O, Ferro M, Coge F, Beauverger P, Henlin JM, Lefoulon F, et al. Identification of the melatonin-binding site MT_3 as the quinone reductase 2. J Biol Chem 2000;275:31311–7.
[14] Nosjean O, Nicolas JP, Klupsch F, Delagrange P, Canet E, Boutin JA. Comparative pharmacological studies of melatonin receptors: MT_1, MT_2 and MT_3/QR2. Tissue distribution of MT_3/QR2. Biochem Pharmacol 2001;61:1369–79.
[15] Pintor J, Martin L, Pelaez T, Hoyle CHV, Peral A. Involvement of melatonin MT_3 receptors in the regulation of intraocular pressure in rabbits. Eur J Pharmacol 2001;416:251–4.
[16] Pintor J, Pelaez T, Hoyle CHV. Peral A. Ocular hypotensive effects of melatonin receptor agonists in the rabbit: further evidence for an MT_3 receptor. Br J Pharmacol 2003;138:831–6.
[17] Serle JB, Wang RF, Peterson WM, Plourde R, Yerxa BR. Effect of 5-MCA-NAT, a putative melatonin MT3 receptor agonist, on intraocular pressure in glaucomatous monkey eyes. J Glaucoma 2004;13:385–8.
[18] Mailliet F, Ferry G, Vella F, Thiam K, Delagrange P, Boutin JA. Organs from mice deleted for NRH:quinone oxydoreductase 2 are deprived of the melatonin binding site MT_3. FEBS Lett 2004;578:116–20.
[19] Dinkova-Kostova AT, Talalay P. Persuasive evidence that quinone reductase type 1 (DT diaphorase) protects cells against the toxicity of electrophiles and reactive forms of oxygen. Free Radic Biol Med 2000;29:231–40.
[20] Long DJ, Iskander K, Gaikwad A, Arin M, Roop DR, Knox R, et al. Disruption of dihydronicotinamide riboside:quinone oxidoreductase 2 (NQO2) leads to myeloid hyperplasia of bone marrow and decreased sensitivity to menadione toxicity. J Biol Chem 2002;277:46131–9.
[21] Pozo D, Reiter RJ, Calvo JR, Guerrero JM. Physiological concentrations of melatonin inhibit nitric oxide synthase in rat cerebellum. Life Sci 1994;55:L455–60.
[22] Reiter RJ, Melchiorri D, Sewerynek E, Poeggeler B, Barlow-Walden L, Chuang J, et al. A review of the evidence supporting melatonin's role as an antioxidant. J Pineal Res 1995;18:1–11.
[23] Barlow-Walden LR, Reiter RJ, Abe M, Pablos M, Menendez-Pelaez A, Chen LD, et al. Melatonin stimulates brain glutathione peroxidase activity. Neurochem Int 1995;26:497–502.
[24] Cabeza J, Motilva V, Martin MJ, de la Lastra CA. Mechanisms involved in gastric protection of melatonin against oxidant stress by ischemia-reperfusion in rats. Life Sci 2001;68:1405–15.
[25] Liao S, Dulanet JT, Williams-Ashman HG. Purification and properties of a flavoprotein catalyzing the oxidation of reduced ribosyl nicotinamide. J Biol Chem 1962;237:2981–7.
[26] Foster CE, Bianchet MA, Talalay P, Faig M, Amzel LM. Structures of mammalian cytosolic quinone reductases. Free Radic Biol Med 2000;29:241–5.
[27] Wu K, Knox R, Sun XZ, Joseph P, Jaiswal AK, Zhang D, et al. Catalytic properties of NAD(P)H:quinone oxidoreductase-2 (NQO2), a dihydronicotinamide riboside dependent oxidoreductase. Arch Biochem Biophys 1997;347:221–8.
[28] Zhao Q, Yang XL, Holtzclaw WD, Talalay P. Unexpected genetic and structural relationships of a long-forgotten flavoenzyme to NAD(P)H:quinone reductase (DT-diaphorase). Proc Natl Acad Sci USA 1997;94:1669–74.
[29] Bianchet MA, Foster C, Faig M, Talalay P, Amzel LM. Structure and mechanism of cytosolic quinone reductases. Biochem Soc Trans 1999;27:610–5.

[30] Foster CE, Bianchet MA, Talalay P, Zhao Q, Amzel LM. Crystal structure of human quinone reductase type 2, a metalloflavoprotein. Biochemistry 1999;38:9881–6.
[31] Kwiek JJ, Haystead TAJ. Rudolph J. Kinetic mechanism of quinone reductase 2 and its inhibition by the antimalarial quinolines. Biochemistry 2004;43:4538–47.
[32] Buryanovskyy L, Fu Y, Boyd M, Ma Y, Hsieh TC, Wu JM, et al. Crystal structure of quinone reductase 2 in complex with resveratrol. Biochemistry 2004;43:11417–26.
[33] Vella F, Ferry G, Delagrange P, Boutin JA. NRH:quinone reductase 2: an, enzyme of surprises and mysteries. Biochem Pharmacol, in press.
[34] Leclerc V, Yous S, Delagrange P, Boutin JA, Renard P, Lesieur D. Synthesis of nitroindole derivatives with high affinity and selectivity for melatoninergic binding sites MT(3). J Med Chem 2002;45:1853–9.
[35] Lesieur D, Klupsch F, Guillaumet G, Viaud MC, Langlois M, Bennejean C, et al. Preparation of heteroarylcarboxylates and analogs as melatonin receptor ligands. International Patent Application WO 9958496 (November 18, 1999).
[36] Wallez V, Durieux-Poissonnier S, Chavatte P, Boutin JA, Audinot V, Nicolas JP, et al. Synthesis and structure–activity relationships of novel benzofuran derivatives as MT(2) melatonin receptor selective ligands. J Med Chem 2002;45:2788–800.
[37] Charton I, Mamai A, Bennejean C, Renard P, Delagrange P, Morgan PJ, et al. Synthesis and biological activity of new melatonin receptor ligands. Pharm Pharmacol Commun 2000;6:49–60.
[38] Viaud MC, Guillaumet G, Mazeas D, Vandepoel H, Renard P, Pfeiffer B, et al. Preparation of N-(pyrrolopyridylalkyl)alkanamides and analogs as melatonin receptor ligands. European Patent EP 737685 (October 16, 1996).
[39] Guillaumet G, Viaud MC, Van De Poel H, Delagrange P, Bennejean C, Renard P. Preparation of polycyclic azaindole derivatives and their affinity for melatonin receptors European Patent EP 1092717 (April 18, 2001).
[40] Bradford M. A rapid and sensitive method for the quantification of micrograms quantities of protein utilizing the principle of protein-dye binding. Anal Biochem 1976;72:248–54.
[41] Scatchard G. The attraction of protein for small molecules and ions. Ann NY Acad Sci 1949;51:660–72.
[42] Cheng YC, Prussof WH. Relationship between the inhibition constant (K_i) and the concentration of inhibitor which causes 50% inhibition (IC_{50}) of an enzymatic reaction. Biochem Pharmacol 1973;22:3099–108.
[43] Boutin JA, Chatelain-Egger F, Vella F, Delagrange P, Ferry G. Quinone reductase 2 substrates, cosubstrates and inhibitors. Chemico-Biol Int 2005;151:213–28.
[44] Teshima K, Kondo T. Analytical method for ubiquinone-9 and ubiquinone-10 in rat tissues by liquid chromatography/turbo ion spray tandem mass spectrometry with 1-alkylamine as an additive to the mobile phase. Anal Biochem 2005;338:12–9.
[45] Suhara Y, Kamao M, Tsugawa N, Okano T. Method for the determination of vitamin K homologues in human plasma using high-performance liquid chromatography–tandem mass spectrometry. Anal Chem 2005;77:757–63.
[46] Boutin JA, Audinot V, Ferry G, Delagrange P. Molecular tools to study melatonin pathways and actions. Trends Pharmacol Sci 2005;26:412–9.
[47] Long DJ, Jaiswal AK. Mouse NRH:quinone oxidoreductase (NQO2): cloning of cDNA and gene- and tissue-specific expression. Gene 2000;252:107–17.
[48] Degli-Esposito M, Ferry G, Masdehors P, Boutin JA, Hickman J, Dive C. Post-translational modification of Bid has differential effects on its susceptibility to cleavage by caspase 8 or caspase 3. J Biol Chem 2003;278:15749–57.
[49] Boutin JA. Myristoylation. Cell Signal 1997;9:15–35.
[50] Colombo S, Longhi R, Alcaro S, Ortuso F, Sprocati T, Flora A, et al. *N*-myristoylation determines dual targeting of mammalian NADH-cytochrome b(5) reductase to ER and mitochondrial membranes by a mechanism of kinetic partitioning. J Cell Biol 2005;168:735–45.